Title:

Aging-related changes in expression and function of glutamate transporters in rat spinal cord astrocytes.

Authors and affiliations:

Shiksha Sharan[1,2,*], Bhanu Prakash Tewari[1,3] and Preeti G. Joshi[1]

1. Department of Biophysics, National Institute of Mental Health and Neurosciences, Hosur main road, Bangalore-560029, India

2. Department of Psychiatry, National Institute of Mental Health and Neurosciences, Hosur main road, Bangalore-560029, India

3. Department of Neuroscience, University of Virginia, Charlottesville. VA-22903, USA.

*** Correspondence:**

Shiksha Sharan, Ph.D., shikshasharan1@gmail.com

Key words: Astrocytes**,** Excitotoxicity, Aging, Glutamate, transporter, spinal cord.

Abstract:

Astrocytes are the most abundant and heterogeneous cells in the CNS. They not only promote neuronal health and survival but also protect neurons from glutamate-induced excitotoxic insults. In the spinal cord, astrocytes are present in both Dorsal Horn (DH) and Ventral Horn (VH) however only motor neurons in the ventral horn are highly vulnerable to glutamate excitotoxicity. We hypothesize that the preferential vulnerability of motor neurons may underlie their spatial confinement into the VH wherein astrocytes are differentially equipped with glutamate handling machinery. With aging, this glutamate excitotoxicity increases suggesting a compromised astrocytic glutamate handling as a function of aging. Our results suggest a global reduction in the numerical density and astroglial coverage of in spinal cord, with the most prominent decline in the ventral horn with aging. Astrocytic glutamate transporter EAAT1 and EAAT2 show an overall reduction in expression with aging. However, the VH showed a progressive decrease compared to the DH. To assess the functional outcome of the

altered expression of EAATs with aging we performed whole-cell patch-clamp studies in DH and VH astrocytes with aging. Both VH and DH astrocytes showed a dramatic decline in the glutamate uptake currents with aging, suggesting a compromised glutamate handling by aging astrocytes. Our study suggests that astrocytes in the dorsal and ventral horn undergo differential changes with aging leading to compromise in their glutamate handling properties. These age and region-associated alterations in extracellular glutamate regulation through astrocytic glutamate transporters may be key contributors to the late onset of neurodegenerative disorders.

1. INTRODUCTION

Astrocytes are the most abundant glial cells in the CNS [5] and play numerous roles including metabolic and trophic support, ion homeostasis, neurotransmitter buffering, and maintaining blood-brain barrier (BBB) integrity [27,32]. Recent studies provide evidence of a dynamic bidirectional interaction between astrocytes and neurons that regulate neuronal activity thereby generating behavioural patterns [38]. One of the major functions of astrocytes is to uptake the excess extracellular glutamate released during the synaptic activity owing to the strategic placement of their fine processes capable of an efficient glutamate clearance at synapses. Although glutamate is the major excitatory neurotransmitter responsible for normal CNS functioning, an abnormally high level of glutamate poses a risk of excitotoxicity, oxidative stress, neuronal hyperexcitability, neuronal death [22], etc., and astrocytes play important roles in maintaining the extracellular glutamate [3].

A combination of 5 Excitatory Amino Acid Transporters (EAAT1-5) expressed in a strategic manner act in concert to remove the excess glutamate with high efficiency [45,53]. The EAAT1/GLAST and EAAT2/GLT1 are located primarily on astrocytes, and EAAT2 alone accounts for approximately 90% of all glutamate transport [3,30,41]. Although EAAT2 is believed to be the major transporter subtype in removing excess glutamate from the synaptic cleft, EAAT1 also plays a critical role in preventing

excitotoxic neuronal injury [42]. The EAAT3 is predominantly expressed by neurons [21]. EAAT4 is also a neuron-specific glutamate transporter, which is specifically expressed by Purkinje cells, and EAAT5 is selectively expressed in the retina [34]. Astroglial dysfunction due to altered EAATs expression contributes to glutamate-induced excitotoxicity and has been implicated in many neurological diseases including seizures [2,43,57], and Amyotrophic lateral sclerosis (ALS) as well as during normal aging [6,15,31,35].

Aging is a key contributor to the progression and aggravation of neurodegenerative diseases like ALS, by increasing the risk factor for neurodegeneration and increasing the severity of the disease [7,29,59]. It has been observed that aged individuals have more severe forms of disease or incomplete recovery after damage [36]. With the normal aging process, a decline in physiological function, increase neuroinflammation, brain shrinkage, and memory deficits have been reported [10,14]. Molecular and cellular changes that occur during aging are known to render neurons vulnerable to excitotoxicity. Studies of mouse models of neurodegenerative diseases support the role of excitotoxicity in these disorders. With aging, astrocytes also undergo changes that significantly lower their ability to support neuronal functions in the brain as well as in the spinal cord [13]. Since most neurodegenerative diseases have a late-onset and neurons are specifically susceptible to glutamate excitotoxicity which can be due to dysfunctional glutamate homeostasis [18,20,28], it is pivotal to understand glutamate handling properties of astrocytes with respect to aging [35].

One of the emerging attributes of astrocytes in recent decades is their structural and functional heterogeneity suggesting that astrocytes are adapted according to the niche where they exist [11]. For example, astrocytes in the ventral horn express high levels of inward rectifying K^+ channel (Kir 4.1) than that of the dorsal horn [40]. Recent studies have shown a differential expression of astrocytic homeostatic proteins such as Kir4.1 around the alpha motor neurons and in the ventral horn [26,40], and disease conditions such as ALS and Huntington's disease dysfunctional K^+ and Glu homeostasis

by astrocytes contribute to the pathology [44,54]. Additionally, in diseases such as ALS, motor neurons of the ventral horn are preferentially susceptible sparing other spinal sensory neurons as shown by several studies including ours [8,24,25,49,56].

A large number of studies have established that spinal sensory and motor neurons residing in the DH and VH respectively not only differ morphologically but also functionally, however evidence of such regional differences in astrocytes and how aging alters astrocytic properties are less explored. In the present study, we investigated whether the properties of astrocytes surrounding motor neurons are different from that of sensory neurons and if this regional difference in astrocytic properties makes motor neurons susceptible to glutamate excitotoxicity. We also examined the astrocytic properties in 3 distinct age groups to address changes associated with normal aging. This study takes advantage of the spinal cord as a model system wherein highly susceptible motor neurons are present in VH and are spatially isolated from less susceptible sensory neurons in DH. This provides advantages to studying the astrocytic milieu surrounding motor neurons and sensory neurons separately without an overlap.

2. RESULTS

2.1. Distinct density and morphology of astrocytes in dorsal and ventral horns of rat spinal cord and changes with age

In the spinal cord, astrocytes ensheath motor and sensory neurons in ventral and dorsal horns respectively. However, only motor neurons are highly vulnerable to glutamate excitotoxicity and with aging, this vulnerability gradually increases with age [29,59]. Since astrocytes are primary cells responsible for clearing the extracellular glutamate, the higher vulnerability of motor neurons may underlie the structural and functional differences in dorsal and ventral horn astrocytes. To this end, first, we assessed the numerical density of astrocytes with aging and whether any differential changes

are occurring between dorsal and ventral horns astrocytes with aging. Using astrocyte-specific marker S100β in transverse spinal cord sections, we observed a remarkably lower number of astrocytes in the spinal cord with aging (Fig. 1A, B). The density of astrocytes was highest in the juvenile spinal cord (131±5; n = 5 rats), which decreased to >50% in young adults (56±3; n = 5 rats) and old (49±2; n = 5 rats) (Fig. 1B).

Next, to ascertain the differences in the astrocytic milieu of sensory and motor neurons with aging, we compared the density of S100β-labelled astrocytes in DH and VH of all age groups. In juvenile rats, VH showed a higher density of astrocytes than the DH (VH 75±4, DH 56±2; n = 5 rats) (Fig. 1A and 1C). Furthermore, in the VH of young adults (DH 41±3, VH 15±1; n = 5 rats) and old groups (DH 32±1; VH 16±0.81; n = 5 rats), a significantly lower number of S100β-positive astrocytes were observed compared to the DH (Fig. 1C). Morphologically, astrocytic processes were less intricate in the juvenile group, however S100β immunofluorescence in the astrocytic processes appreciably increased in the young adult and old groups and the processes appeared more elaborate and profusely surrounding the neurons in the DH as well as VH (Fig.1A white arrows). This data suggests that the VH possesses a higher density of astrocytes than DH at an early age, however with aging, the total number of astrocytes decreases in both regions with a more severe decline in the VH than the DH.

Since astrocytes mature morphologically with the development which involves an increase in astrocytic arborizations and astrocytic coverage [55], we assessed whether or not a decline in the astrocytic numbers affects the overall glial coverage in the spinal cord. The high numerical density of astrocytes in the juvenile age (Fig. 1B) showed the lowest glial coverage (Fig. 1D 37±9, n = 3 rats) which increased to ~48 fold in young adults (Fig. 1D 456±17, n = 4 rats) and subsequently reduced significantly at the old age (Fig. 1D 309±36, n = 4 rats). In the DH and VH, astrocytic coverage showed a similar increase from juvenile (Fig. 1E DH 21±7, VH 53±14, n = 3 rats) to the young adult (Fig. 1E DH 430±29, VH 481±8, n = 4 rats) however only DH showed a significant decline in the old group

(Fig. 1E DH 193±77, VH 426±20, n = 4 rats). These data suggest that although the numerical density of astrocytes decreases with age, however, the glial coverage appears to remain stable and decreases only in DH in old age.

2.2 Change in expression of astrocytic glutamate transporters EAAT1 and EAAT2 in the spinal cord with age

Next, we assessed whether astrocytes surrounding the motor and sensory neurons have a differential glutamate transporter expression and does this expression changes with aging. First, we examined changes in overall expression levels of EAAT1 and EAAT2 in the spinal cord with aging by performing a western blot analysis from the lumbar region of spinal cord tissue. Since EAATs are extensively characterized in the hippocampal astrocytes, we used hippocampal tissue as a positive control for the transporter expression. Consistent with earlier reports [39] the protein bands corresponding to EAAT1 and EAAT2, were detected at 60 kD and 65-67 kD respectively (Fig. 2 A-B; Fig. 3 A-B).

In the spinal cord EAAT1 expression was highest in the juvenile group (Fig. 2A, D 33±4, n = 3 rats) and reduced with increasing age but without any statistical significance in young adults (Fig. 2A, D 21±5, n =3 rats) and old groups (Fig. 2A, D 22±3, n = 3 rats). However, the positive control hippocampus also showed the highest EAAT1 expression in juveniles which significantly declined with increasing age (Fig. 2A, D juvenile 46±8; young adult 37±5; old 26±0.8, n = 3 rats) suggesting a CNS region independent change in EAAT1 expression with aging. Next, we compared the EAAT1 expression in DH and VH and observed that in the juvenile group the EAAT1 expression was significantly lower in the VH as compared to DH (Fig. 2B, E juvenile DH 164±40; VH 116±13 n =3 rats). With the progression of age, the EAAT1 expression decreased significantly in the DH, however, VH remained unchanged (Fig. 2B, E young adult DH 113±7; VH 101±9; old DH 125±14, VH 124±17 n = 3 rats).

To further confirm the distribution and differential expression of EAAT1 with aging and in DH and VH, we assessed the immunofluorescence of EAAT1 in the spinal cord transverse sections at the lumber level. EAAT1 immunofluorescence showed a distinct pattern in DH wherein rexed lamina II/III/IV of DH especially in young adult and old groups showed the most intense expression (Fig. 2Coutlined). VH on the other hand showed nearly uniform expression, although in higher aged groups astrocytes appear to border the cell body of motor neurons. In young adult and old age groups, the EAAT1 expression was significantly lower in the VH as compared to DH and the difference was more prominent in the old age (Fig. 2 C, F young adult DH 100±11, VH 52±9; old DH 100±9, VH 35±4, n = 4 rats).

The expression of EAAT2, which accounts for 90% of glutamate transport in astrocytes [50] showed a decline with the progression of age in the spinal cord. There was a 3-fold higher expression of EAAT2 in the juvenile group (Fig 3D 75±21, n = 3 rats) compared to the young adult (Fig 3D 19±2, n = 3 rats). There was no significant difference in EAAT2 expression between old group and young adult group (Fig 3D old 38±4, n = 3 rats). While, in the positive control hippocampus the EAAT2 expression was highest in the young adult group as compared to other age groups (Fig 3D juvenile 93±19; young adult 163±20; old 95±27, n = 3 rats).

Subsequently, we compared the EAAT2 expression in DH and VH and observed that in the juvenile group the EAAT2 expression was higher in VH than in DH (Fig 3E DH 60±3; VH 87±12, n = 3 rats). EAAT2 expression decreased in higher age groups with a much lower expression in the VH than the DH (Fig 3E young adult DH 66±10; VH 46±3; old DH 38±5; VH 26±3 n = 3 rats). Overall, these data suggest an explicit decrease in the EAAT2 level with age, notably in the VH. However, DH had comparable EAAT2 expression in juvenile and young adult groups, with old animals having the least EAAT2 expression (Fig. 3E).

The immunohistochemistry data showed comparable EAAT2 expression in DH and VH of juvenile groups. However, VH of the young adult and old group had higher EAAT2 expression in VH than DH (Fig. 3 C, F old DH 100±10; VH 62±9, n = 4 rats).

Collectively, both EAAT1 and EAAT2 displayed different regional distribution patterns that varied moderately among the three age groups (juvenile, young adult, and old). EAAT1 immunoreactivity was found to be more in lamina II as compared to other laminas of the spinal cord (Fig. 2C, outlined). However, EAAT2 was more intense in lamina III, IV, and V as compared to lamina I and II, especially in young adult and old rats (Fig. 3C, outlined). Both EAAT1 and EAAT2 were mostly uniformly distributed in VH of the spinal cord with more prominent expression in the surroundings of motor neurons (Fig-2C and 3C). The expression of EAAT1 and EAAT2 showed an overall decline in the spinal cord with aging, however ventral horn showed a more severe decline than dorsal horn astrocytes suggesting a lower glutamate uptake capacity of ventral horn astrocytes with aging.

2.3 Glutamate uptake in DH and VH astrocytes with aging

To assess the glutamate uptake by astrocytes, we measured glutamate-induced current in DH and VH astrocytes in ex-situ spinal cord acute slices. Astrocytes were identified and selected based on morphology, size, location, and electrophysiological properties [37,60]. The resting membrane potential in astrocytes was in the range of -68 mV to -70 mV (n=22) as opposed to -60 mV to -63 mV in neurons (n=3). In the current clamp mode, injection of a 20 pA current for 100 ms induced a train of action potentials in the neurons whereas the astrocytes exhibited a passive depolarization (Fig. S2). We used glutamate current recordings from hippocampal astrocytes as a positive control.

For all the glutamate uptake current recordings in astrocytes, the membrane potential was held at -70 mV and a 10 mM glutamate pulse was applied for 1 minute by superfusion system. Fig. 4A shows the representative traces of currents recorded from astrocytes of DH, VH, and hippocampus in

all three age groups. The astrocytes in the juvenile group exhibited considerable glutamate uptake currents which were comparable in DH and VH (Fig. 4B, DH 171±33 pA; VH 155±25, n = 12 cells, from 6 rats) astrocytes. We observed a significant decline in glutamate uptake current, both in DH and VH of young adults (Fig. 4B, DH 15±4 pA; VH 13±5, n = 5 cells, from 5 rats) and old groups (Fig. 4B, DH 10±5 pA; VH 10±3, n = 5 cells, from 5 rats).

For these experiments, hippocampal astrocytes from the CA1 region were taken as an age-matched positive control, and glutamate uptake current was measured in all three age groups. Earlier studies have reported a decline in astrocytic glutamate uptake current with maturing [46]. Our data also confirmed a substantial decline in the astrocytic glutamate uptake current with aging in the hippocampus (Fig. 4C, juvenile 335±39 pA n = 6 cells; young adult 153±28 n = 4 cells; old 110±26 n = 6 cells, from 4 rats). However, the uptake current recorded in the astrocytes of the hippocampus was much higher than in the spinal cord astrocytes. In the hippocampus, as compared to the juvenile group, higher age groups showed approximately a 67% decrease in glutamate uptake current. Contrary to this, in the spinal cord the glutamate uptake current declined drastically to 93% in higher age groups, with comparable uptake current in young adult and old rats.

3. DISCUSSION

It is well known that the degeneration of neurons occurs during normal aging and the onset of neurodegenerative disorders is typically superimposed with aging [4,59]. Glutamate-induced excitotoxicity has been implicated in age-related degeneration of neurons as well as in several neurodegenerative disorders. Recent studies have shown that astrocytes undergo senescence and contribute to aging and disease [9,47]. Das and Svendsen (2015) have reported that spinal cord astrocytes derived from aged rats and $SOD1^{93A}$ mutant rats show senescence phenotype and possess a lower capacity to support motor neurons [13]. These studies were performed in the astrocyte cultures derived from rat spinal cord and their influence on the survival of co-cultured NSC34 motor neuron

cells, was assessed. Therefore, these studies do not mimic the neuron-astrocyte interaction in situ or in vivo, the in-vivo studies are largely absent in this field. In our study, we have assessed the effects of aging on characteristics of astrocytes in-situ, which may influence the neuron-astrocyte interaction in the spinal cord. The characteristics of astrocytes residing in the VH, and DH of the spinal cord were examined with special reference to glutamate transporters. In addition, the influence of aging on astrocyte characteristics was examined. Our data show age-related changes in astrocytes which are considered unfavourable for the survival of neurons, and these changes are generally more prominent in the astrocytes surrounding the motor neurons in the VH of the spinal cord.

With the progression of age, the lumbar spinal cord slices showed fewer S100β-labelled astrocytes in the old age group suggesting a decrease in the density of astrocytes. The changes were prominent in the ventral horn. Area analysis of S100β positive astrocytes demonstrated that with increasing age astrocytic coverage also increases this can be due to the age-related mild astrocytic hypertrophy without any concurrent pathology [17]. The hypertrophy observed in aging doesn't mimic the astrogliosis seen in the young brain following injury [16,51,58]. Upon activation, astrocytes secrete factors that modulate neuron survival; activated astrocytes produce neurotrophic factors that promote neuronal growth [1].

Age-related alterations in glutamate management by astrocytes

Many studies have been performed on the expression and function of glutamate transporters in the brain, but little information is available on glutamate transport in the spinal cord. Furuta, A., (1997) studied the glutamate transporter expression in CNS during development. It was shown that the expression of glutamate transporter subtypes alters during development (from E15 to P24) [19]. There are no reports on the expression of glutamate transporter proteins and their activity in the spinal cord in aged animals. Our data show glutamate transporter expression declines with aging in spinal cord astrocytes and more so in the ventral horn. The glial glutamate transporters EAAT1 and EAAT2

expression were observed in both regions of the spinal cord in all age groups but with a distinct decline with aging. Also, the expression of both the transporters was much less in the ventral horn as compared to the dorsal horn.

We measured the glutamate-induced current in astrocytes using the whole cell patch clamp technique. Astrocytes in the juvenile group showed a considerable glutamate uptake current, however, it was significantly lower than the glutamate uptake current observed in the age-matched hippocampus. The glutamate uptake current was suppressed with aging both in the hippocampus as well as the spinal cord. A decrease in the expression of the glial glutamate transporters EAAT1, and EAAT2 and reduced glutamate uptake occur in the aged Sprague Dawley rat hippocampus. Similar results have been reported in the hippocampal striatum where glutamate clearance was compromised in the aged brain [39]. These differences in glutamate uptake current may reflect either differing demands on glutamate homeostasis or compromised glutamate handling capability with aging. A great deal of evidence suggests that glutamate uptake into astrocytes occurs through sodium-dependent excitatory amino acid transporters (EAAT) and studies have shown that the majority of glutamate uptake is through astrocytic glutamate transporter EAAT2 [3,30]. Interestingly, the decline in glutamate uptake current was more dramatic in the spinal cord. As compared to the juvenile group the uptake current was at least ten times lower in young adult and older rats (Fig. 4). Nevertheless, there was appreciable glutamate transporter expression in the old age group. Different studies have demonstrated that elevation of intracellular glutamate and Na ion, results in a decrease of glutamate transporter current in astrocytes [12]. The glutamine synthase (GS) activity in astrocytes dynamically regulates the intracellular glutamate concentration [48] and thus influences the glutamate transport across the membrane. Souza, D.G., et al., (2015) have reported that astrocytic GS activity is decreased in adult and old rats [52]. However, in our study, the glutamate uptake current was measured under the whole cell current clamp conditions, and the intracellular glutamate concentrations under given

experimental conditions would be similar in all age groups therefore the observed decline in glutamate uptake current in the old age group are less likely due to above factors.

In essence, our study provides evidence of impaired glutamate management by astrocytes with aging. The salient role of astrocytes in maintaining extracellular glutamate at synaptic cleft is well known. The present study indicates compromised glutamate uptake capacity of astrocytes with aging as both the transporter expression and glutamate uptake capacity declined with age. Additionally, we reported differential morphological and functional properties of DH and VH spinal astrocytes. Since we have observed a decrease in astrocytic glutamate transporter expression with aging, especially in the VH, it will be interesting to delineate molecular mechanisms regulating the expression of astrocytic glutamate transporters with aging which can be pivotal in understanding the higher risk of certain neurodegenerative diseases with aging.

4. MATERIALS AND METHODS

4.1 Materials

Polyclonal antibodies Anti-EAAT1, and Anti-EAAT2, were obtained from Alomone Laboratories, Jerusalem, Israel. Secondary antibodies Alexa fluor 488 goat anti-rabbit IgG, Alexa fluor 633 goat anti-rabbit, Alexa fluor 633 goat anti-mouse, and Alexa fluor 488 goat-anti mice were purchased from Molecular Probes, Invitrogen, Life Technologies, India. Neurochrom-cy3 conjugated, anti-GFAP-488 conjugated, Guinea pig anti-EAAT2, FITC goat anti-Guinea pig and FITC rabbit anti-goat antibodies were from Merk, Millipore India. Horseradish peroxidase (HRP) conjugated anti-rabbit, anti-mouse antibodies, and L-Glutamate were from Sigma Aldrich. S100β was from Santacruz Biotechnology. For western blotting, Anti EAAT1, β-actin, and tubulin were from Abcam. All other chemicals were analytical grade and were obtained from commercial sources.

4.2 Experimental Animals

Sprague-Dawley rats of three age groups juvenile (21 days), young adult (3 months), and old (20 months) used in this study were obtained from the Central Animal Research Facility of the National Institute of Mental Health and Neurosciences, Bangalore, India. All procedures with animals were carried out according to the guidelines of the institutional animal ethics committee.

4.3 Western blotting

Whole-cell membrane fractions were prepared from the dorsal horn and ventral horn of spinal cord tissue (lumbar region), isolated from different experimental groups. In brief, rats of different age groups were anesthetized and decapitated, the spinal cord was quickly removed by hydraulic extraction. A 60 ml syringe with an 11-gauge needle (blunted tip) filled with Artificial CSF (aCSF) was inserted spinal canal near the L5 segment (1 cm deep). aCSF was injected forcefully to flush out the spinal cord. The cauda equina is identified and the alignment of the spinal cord was done accordingly (rostral end and caudal end). The lumbar part of the spinal cord was isolated and placed in an ice-cold HEPES buffer for 1-2 minutes. Afterward, the spinal cord was sliced to 800 µm thickness and the dorsal horn was separated from the ventral horn by making a horizontal slice at the plane of the central canal using a stereomicroscope. Separated DH and VH were manually homogenized using motor and piston homogenizer in lysis buffer [(in mM) 10 Tris, 5 KCl, 1 DTT, 1 EGTA, and Complete Protease Inhibitor Cocktail (Abcam)], and cell lysate was sonicated.

Protein concentration was determined by Lowry method [33], samples were then diluted 1:1 in sample treatment buffer [(in mM) 25mM Tris, 8% SDS, 40% Glycerol, 0.05 % Bromophenol Blue, 20% β Mercaptoethanol]. After denaturation by heating at 95°C for 3-5 min, 100 µg of protein was loaded in each lane of a 10 % SDS-PAGE gel. Equal concentrations of proteins from both regions were loaded in each well and analysed via electrophoresis. Nonspecific sites were blocked with 5% non-fat milk, and blots were incubated for 3 hrs at Room Temperature (RT) with rabbit polyclonal anti-EAAT1/anti-EAAT2 (1:200) and β-actin/tubulin (1:10000). Blots were then probed with

horseradish peroxidase-conjugated anti-rabbit (1:250) or anti-mouse (1:500) secondary antibodies using Super Signal® West Pico chemiluminescent substrate. The enhanced chemiluminescence was captured using a camera attached to a computer-assisted gel documentation system (Syngene, U.K). Quantification of the band intensities was carried out using Image J software (NIH, USA).

4.4 Immunohistochemistry

Immunohistochemistry (IHC) was performed on free-floating spinal cord sections using the following primary antibodies: rabbit anti-EAAT1 (1:50), Guinea pig anti-EAAT2 (1:1000), mouse anti-GFAP (1:400), mouse anti-S100β (1:100). Transcranial perfusion was done with chilled 0.9% saline followed by 4% paraformaldehyde in PBS. The lumbar region of the spinal cord was taken out and kept in PFA solution for 48 hrs at 4°C and transferred to PBS for further 24 hours at 4°C. 70µm thick sections were prepared using vibratome (Vibratome, 3000 Sectioning System). Antigen retrieval was performed by placing sections in saline sodium citrate and formamide (1:1 by volume) solution (pH 6.4) for 2 hrs at 65°C with gentle shaking in a water bath. Non-specific antigen blocking and permeabilization were done by incubating sections in PBS containing 5% bovine serum albumin, 5% goat serum, and 0.1% Triton X-100, at RT for 2 hrs. Sections were rinsed with PBS and were placed in 100µl of PBS containing the primary antibody, 5% goat serum, and 5% bovine serum albumin for 12 hours at 4°C. Sections were rinsed 5 times with PBS and Alexa fluor-488/633 conjugated or FITC conjugated secondary antibody was added for 6 hours in dark at RT. Sections were rinsed thoroughly with PBS and mounted on gelatin-coated slides using a mounting solution containing 50% glycerol and 50% PBS by volume. Images were acquired using a laser scanning confocal microscope Olympus FV 1000 (Olympus Japan).

4.5 Quantification of receptor expression

For the immunofluorescence analysis of EAAT1 and EAAT2, images were acquired from the dorsal horn and ventral horn of all three age groups. Minimum 3 spinal cord sections from 3 different animals

in each age group were taken for analysis. Image acquisition parameters were kept constant for all age groups. Uniform-sized ROIs were drawn in the specific spinal cord area of all the groups and the average fluorescence intensity was obtained using Fluo-view software (Olympus, Japan). The ventral horn percentages are calculated concerning the dorsal horn normalized to 100% [23]. Data representing the mean ± SEM, was compared in different experimental groups

4.6 Quantification of astrocytic numerical density and coverage

S100β-labelled spinal cord sections were used for quantitative analysis of astrocytic coverage present in the spinal cord of different age groups. The distribution of astrocytes in the dorsal and ventral horn and whole spinal cord was analyzed and compared in different age groups. Cell counting and area analysis was performed on the confocal microscope acquired images using ImageJ NIH image analysis software (http://rsb.info.nih.gov/ij/download.html). For cell counting, the acquired image was converted into an 8-bit binary image, and a threshold was set. The cells were counted using an overlay of the original and the binary image. For astrocytic coverage, we calculated the total area of astrocytes using an automated binary thresholding method in imageJ. The area acquired by cells was measured and analyzed.

4.7 Acute slice preparation for whole-cell patch-clamp recording

Transverse slices from the lumbar region of the spinal cord and coronal brain slices (300 µm) enclosing the hippocampus were prepared from deeply anesthetized SD rats from specific age groups using a vibratome (Vibratome, 3000 Sectioning System). The brain/spinal cord was rapidly removed and placed in an ice-cold cutting buffer (in mM): 215 Sucrose, 2.5 KCl, 1.25 NaH_2PO_4, 0.5 $CaCl_2$, 4 $MgSO_4.7H_2O$, 26.2 $NaHCO_3$, 1 Ascorbate, equilibrated with a mixture of 95% O_2 and 5% CO_2. The tissue was glued to the slicing stage of a Leica vibratome. Slices were incubated in oxygenated minimum essential medium eagle (MEM) for 1 hour at room temperature (RT). Subsequent whole-cell patch-clamp recordings were performed at room temperature. Resistances of the patch pipettes

were typically 6-8 MΩ (P-2000, Sutter Instruments, USA). The pipette solution contained (in mM): 145 potassium gluconate, 5 NaCl, 2 $MgCl_2$, 10 HEPES, 0.2 EGTA. Cells were visualized with infrared optics on an upright microscope (Eclipse E600-FN Nikon) (Fig. S1). Astrocytes were identified and selected on basis of their size, location, and electrophysiological properties. Inward currents were recorded at -70 mV [40] using Patchmaster software, EPC10 amplifier, HEKA, Germany. Data was filtered at 10 kHz (Bessel filter) and compensated for C-fast and C-slow. L-glutamate (10 mM) was applied by superfusion without an alteration of the perfusion rate and temperature.

4.8 Statistical Analysis

Statistical analysis was done using OriginPro or SigmaPlot programs and data are reported as mean ± SEM. In experiments, an unpaired *t*-test was used to assess the significance between two groups, and with more than two groups, the assessment was done by One-Way ANOVA followed by the Fisher LSD *posthoc* test. The threshold for statistical significance was set at $p \leq 0.05$. In the figures, * represents $p \leq 0.05$, ** represents $p \leq 0.01$ and *** represents $p \leq 0.001$.

Abbreviations: DH: Dorsal Horn, VH: Ventral Horn, CA1: Cornu Ammonis 1, EAAT1: Excitatory Amino Acid Transporter 1, EAAT2: Excitatory Amino Acid Transporter 1

Author's contribution:

Shiksha Sharan: Conceptualization, conducted experiments, methodology, data curation, visualization, Investigation, validation, writing original draft and reviewing; **Bhanu Prakash Tiwari**: Methodology, writing, reviewing, editing; **Preeti G. Joshi:** supervision, conceptualization, visualization, methodology, validation.

Acknowledgments:

Animal facility: Central Animal Research Facility, National Institute of Mental Health & Neurosciences, Bangalore, India. Funding: SS received a fellowship from the Department of Science and Technology, Government of India.

Conflict of interest:

None

Funding:

This study is supported by Department of science and technology, New Delhi, India

References:

[1] Albrecht PJ, Dahl JP, Stoltzfus OK, Levenson R, Levison SW. Ciliary neurotrophic factor activates spinal cord astrocytes, stimulating their production and release of fibroblast growth factor-2, to increase motor neuron survival. Exp Neurol 2002;173(1):46-62.

[2] Alcoreza OB, Patel DC, Tewari BP, Sontheimer H. Dysregulation of Ambient Glutamate and Glutamate Receptors in Epilepsy: An Astrocytic Perspective. Front Neurol 2021;12:652159.

[3] Anderson CM, Swanson RA. Astrocyte glutamate transport: review of properties, regulation, and physiological functions. Glia 2000;32(1):1-14.

[4] Azam S, Haque ME, Balakrishnan R, Kim IS, Choi DK. The Ageing Brain: Molecular and Cellular Basis of Neurodegeneration. Front Cell Dev Biol 2021;9:683459.

[5] Belanger M, Allaman I, Magistretti PJ. Brain energy metabolism: focus on astrocyte-neuron metabolic cooperation. Cell Metab 2011;14(6):724-38.

[6] Bronzuoli MR, Facchinetti R, Valenza M, Cassano T, Steardo L, Scuderi C. Astrocyte Function Is Affected by Aging and Not Alzheimer's Disease: A Preliminary Investigation in Hippocampi of 3xTg-AD Mice. Front Pharmacol 2019;10:644.

[7] Broussalis E, Grinzinger S, Kunz AB, Killer-Oberpfalzer M, Haschke-Becher E, Hartung HP, Kraus J. Late age onset of amyotrophic lateral sclerosis is often not considered in elderly people. Acta Neurol Scand 2018;137(3):329-34.

[8] Carriedo SG, Sensi SL, Yin HZ, Weiss JH. AMPA exposures induce mitochondrial Ca(2+) overload and ROS generation in spinal motor neurons in vitro. J Neurosci 2000;20(1):240-50.

[9] Chinta SJ, Lieu CA, Demaria M, Laberge RM, Campisi J, Andersen JK. Environmental stress, ageing and glial cell senescence: a novel mechanistic link to Parkinson's disease? J Intern Med 2013;273(5):429-36.

[10] Chung HY, Kim DH, Lee EK, Chung KW, Chung S, Lee B, Seo AY, Chung JH, Jung YS, Im E, Lee J, Kim ND, Choi YJ, Im DS, Yu BP. Redefining Chronic Inflammation in Aging and Age-Related Diseases: Proposal of the Senoinflammation Concept. Aging Dis 2019;10(2):367-82.

[11] Clarke BE, Taha DM, Tyzack GE, Patani R. Regionally encoded functional heterogeneity of astrocytes in health and disease: A perspective. Glia 2021;69(1):20-7.

[12] Danbolt NC. Glutamate uptake. Prog Neurobiol 2001;65(1):1-105.

[13] Das MM, Svendsen CN. Astrocytes show reduced support of motor neurons with aging that is accelerated in a rodent model of ALS. Neurobiol Aging 2015;36(2):1130-9.

[14] Esiri MM. Ageing and the brain. J Pathol 2007;211(2):181-7.

[15] Farrand AQ, Gregory RA, Scofield MD, Helke KL, Boger HA. Effects of aging on glutamate neurotransmission in the substantia nigra of Gdnf heterozygous mice. Neurobiol Aging 2015;36(3):1569-76.

[16] Faulkner JR, Herrmann JE, Woo MJ, Tansey KE, Doan NB, Sofroniew MV. Reactive astrocytes protect tissue and preserve function after spinal cord injury. J Neurosci 2004;24(9):2143-55.
[17] Finch CE. Neurons, glia, and plasticity in normal brain aging. Neurobiol Aging 2003;24 Suppl 1:S123-7; discussion S31.
[18] Foran E, Trotti D. Glutamate transporters and the excitotoxic path to motor neuron degeneration in amyotrophic lateral sclerosis. Antioxid Redox Signal 2009;11(7):1587-602.
[19] Furuta A, Rothstein JD, Martin LJ. Glutamate transporter protein subtypes are expressed differentially during rat CNS development. J Neurosci 1997;17(21):8363-75.
[20] Gasiorowska A, Wydrych M, Drapich P, Zadrozny M, Steczkowska M, Niewiadomski W, Niewiadomska G. The Biology and Pathobiology of Glutamatergic, Cholinergic, and Dopaminergic Signaling in the Aging Brain. Front Aging Neurosci 2021;13:654931.
[21] Holmseth S, Dehnes Y, Huang YH, Follin-Arbelet VV, Grutle NJ, Mylonakou MN, Plachez C, Zhou Y, Furness DN, Bergles DE, Lehre KP, Danbolt NC. The density of EAAC1 (EAAT3) glutamate transporters expressed by neurons in the mammalian CNS. J Neurosci 2012;32(17):6000-13.
[22] Iovino L, Tremblay ME, Civiero L. Glutamate-induced excitotoxicity in Parkinson's disease: The role of glial cells. J Pharmacol Sci 2020;144(3):151-64.
[23] Jones J, Estirado A, Redondo C, Martinez S. Stem cells from wildtype and Friedreich's ataxia mice present similar neuroprotective properties in dorsal root ganglia cells. PLoS One 2013;8(5):e62807.
[24] Joshi DC, Singh M, Krishnamurthy K, Joshi PG, Joshi NB. AMPA induced Ca2+ influx in motor neurons occurs through voltage gated Ca2+ channel and Ca2+ permeable AMPA receptor. Neurochem Int 2011;59(6):913-21.
[25] Joshi DC, Tewari BP, Singh M, Joshi PG, Joshi NB. AMPA receptor activation causes preferential mitochondrial Ca^{2+} load and oxidative stress in motor neurons. Brain Res 2015;1616:1-9.
[26] Kelley KW, Ben Haim L, Schirmer L, Tyzack GE, Tolman M, Miller JG, Tsai HH, Chang SM, Molofsky AV, Yang Y, Patani R, Lakatos A, Ullian EM, Rowitch DH. Kir4.1-Dependent Astrocyte-Fast Motor Neuron Interactions Are Required for Peak Strength. Neuron 2018;98(2):306-19.e7.
[27] Kim Y, Park J, Choi YK. The Role of Astrocytes in the Central Nervous System Focused on BK Channel and Heme Oxygenase Metabolites: A Review. Antioxidants (Basel) 2019;8(5).
[28] King AE, Woodhouse A, Kirkcaldie MT, Vickers JC. Excitotoxicity in ALS: Overstimulation, or overreaction? Exp Neurol 2016;275 Pt 1:162-71.
[29] Le Gall L, Anakor E, Connolly O, Vijayakumar UG, Duddy WJ, Duguez S. Molecular and Cellular Mechanisms Affected in ALS. J Pers Med 2020;10(3).
[30] Lehre KP, Danbolt NC. The number of glutamate transporter subtype molecules at glutamatergic synapses: chemical and stereological quantification in young adult rat brain. J Neurosci 1998;18(21):8751-7.
[31] Lewerenz J, Maher P. Chronic Glutamate Toxicity in Neurodegenerative Diseases-What is the Evidence? Front Neurosci 2015;9:469.
[32] Liddelow SA, Guttenplan KA, Clarke LE, Bennett FC, Bohlen CJ, Schirmer L, Bennett ML, Münch AE, Chung WS, Peterson TC, Wilton DK, Frouin A, Napier BA, Panicker N, Kumar M, Buckwalter MS, Rowitch DH, Dawson VL, Dawson TM, Stevens B, Barres BA. Neurotoxic reactive astrocytes are induced by activated microglia. Nature 2017;541(7638):481-7.
[33] Lowry OH, Rosebrough NJ, Farr AL, Randall RJ. Protein measurement with the Folin phenol reagent. J Biol Chem 1951;193(1):265-75.

[34] Magi S, Piccirillo S, Amoroso S, Lariccia V. Excitatory Amino Acid Transporters (EAATs): Glutamate Transport and Beyond. Int J Mol Sci 2019;20(22).
[35] Mattson MP, Magnus T. Ageing and neuronal vulnerability. Nat Rev Neurosci 2006;7(4):278-94.
[36] Mayne K, White JA, McMurran CE, Rivera FJ, de la Fuente AG. Aging and Neurodegenerative Disease: Is the Adaptive Immune System a Friend or Foe? Front Aging Neurosci 2020;12:572090.
[37] McNeill J, Rudyk C, Hildebrand ME, Salmaso N. Ion Channels and Electrophysiological Properties of Astrocytes: Implications for Emergent Stimulation Technologies. Front Cell Neurosci 2021;15:644126.
[38] Nagai J, Yu X, Papouin T, Cheong E, Freeman MR, Monk KR, Hastings MH, Haydon PG, Rowitch D, Shaham S, Khakh BS. Behaviorally consequential astrocytic regulation of neural circuits. Neuron 2021;109(4):576-96.
[39] Nickell J, Salvatore MF, Pomerleau F, Apparsundaram S, Gerhardt GA. Reduced plasma membrane surface expression of GLAST mediates decreased glutamate regulation in the aged striatum. Neurobiol Aging 2007;28(11):1737-48.
[40] Olsen ML, Campbell SL, Sontheimer H. Differential distribution of Kir4.1 in spinal cord astrocytes suggests regional differences in K+ homeostasis. J Neurophysiol 2007;98(2):786-93.
[41] Ortega A. glutamate transporters: critical components of glutametergic transmission neuropharmacology 2021.
[42] Pajarillo E, Rizor A, Lee J, Aschner M, Lee E. The role of astrocytic glutamate transporters GLT-1 and GLAST in neurological disorders: Potential targets for neurotherapeutics. Neuropharmacology 2019;161:107559.
[43] Peterson AR, Binder DK. Astrocyte Glutamate Uptake and Signaling as Novel Targets for Antiepileptogenic Therapy. Front Neurol 2020;11:1006.
[44] Phatnani H, Maniatis T. Astrocytes in neurodegenerative disease. Cold Spring Harb Perspect Biol 2015;7(6).
[45] Pines G, Danbolt NC, Bjoras M, Zhang Y, Bendahan A, Eide L, Koepsell H, Storm-Mathisen J, Seeberg E, Kanner BI. Cloning and expression of a rat brain L-glutamate transporter. Nature 1992;360(6403):464-7.
[46] Popov A, Brazhe A, Denisov P, Sutyagina O, Li L, Lazareva N, Verkhratsky A, Semyanov A. Astrocyte dystrophy in ageing brain parallels impaired synaptic plasticity. Aging Cell 2021;20(3):e13334.
[47] Salminen A, Ojala J, Kaarniranta K, Haapasalo A, Hiltunen M, Soininen H. Astrocytes in the aging brain express characteristics of senescence-associated secretory phenotype. Eur J Neurosci 2011;34(1):3-11.
[48] Schousboe A, Scafidi S, Bak LK, Waagepetersen HS, McKenna MC. Glutamate metabolism in the brain focusing on astrocytes. Adv Neurobiol 2014;11:13-30.
[49] Sen I, Joshi DC, Joshi PG, Joshi NB. NMDA and non-NMDA receptor-mediated differential Ca2+ load and greater vulnerability of motor neurons in spinal cord cultures. Neurochem Int 2008;52(1-2):247-55.
[50] Sheldon AL, Robinson MB. The role of glutamate transporters in neurodegenerative diseases and potential opportunities for intervention. Neurochem Int 2007;51(6-7):333-55.
[51] Sofroniew MV. Reactive astrocytes in neural repair and protection. Neuroscientist 2005;11(5):400-7.
[52] Souza DG, Bellaver B, Raupp GS, Souza DO, Quincozes-Santos A. Astrocytes from adult Wistar rats aged in vitro show changes in glial functions. Neurochem Int 2015;90:93-7.

[53] Storck T, Schulte S, Hofmann K, Stoffel W. Structure, expression, and functional analysis of a Na(+)-dependent glutamate/aspartate transporter from rat brain. Proc Natl Acad Sci U S A 1992;89(22):10955-9.
[54] Tong X, Ao Y, Faas GC, Nwaobi SE, Xu J, Haustein MD, Anderson MA, Mody I, Olsen ML, Sofroniew MV, Khakh BS. Astrocyte Kir4.1 ion channel deficits contribute to neuronal dysfunction in Huntington's disease model mice. Nat Neurosci 2014;17(5):694-703.
[55] Torres-Ceja B, Olsen ML. A closer look at astrocyte morphology: Development, heterogeneity, and plasticity at astrocyte leaflets. Curr Opin Neurobiol 2022;74:102550.
[56] Van Den Bosch L, Van Damme P, Bogaert E, Robberecht W. The role of excitotoxicity in the pathogenesis of amyotrophic lateral sclerosis. Biochim Biophys Acta 2006;1762(11-12):1068-82.
[57] Verhoog QP, Holtman L, Aronica E, van Vliet EA. Astrocytes as Guardians of Neuronal Excitability: Mechanisms Underlying Epileptogenesis. Front Neurol 2020;11:591690.
[58] Voskuhl RR, Peterson RS, Song B, Ao Y, Morales LB, Tiwari-Woodruff S, Sofroniew MV. Reactive astrocytes form scar-like perivascular barriers to leukocytes during adaptive immune inflammation of the CNS. J Neurosci 2009;29(37):11511-22.
[59] Wyss-Coray T. Ageing, neurodegeneration and brain rejuvenation. Nature 2016;539(7628):180-6.
[60] Zhong S, Du Y, Kiyoshi CM, Ma B, Alford CC, Wang Q, Yang Y, Liu X, Zhou M. Electrophysiological behavior of neonatal astrocytes in hippocampal stratum radiatum. Mol Brain 2016;9:34.

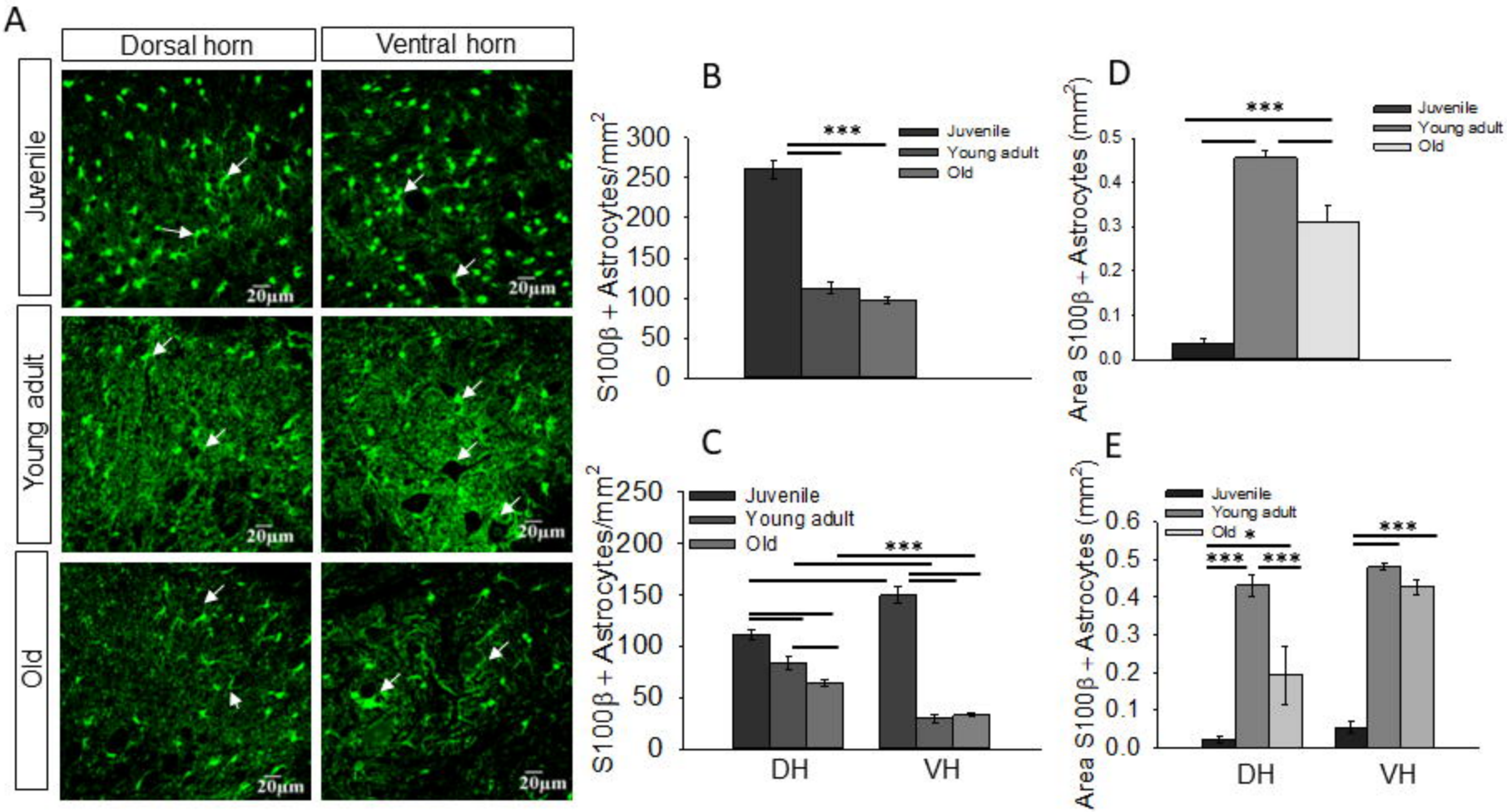
A
Dorsal horn
Ventral horn
Juvenile
Young adult
Old
20µm
B
S100β + Astrocytes/mm2
300
250
200
150
100
50
0
***
Juvenile
Young adult
Old
C
S100β + Astrocytes/mm2
250
200
150
100
50
0
Juvenile
Young adult
Old
***
DH
VH
D
Area S100β + Astrocytes (mm2)
0.5
0.4
0.3
0.2
0.1
0.0
***
Juvenile
Young adult
Old
E
Area S100β + Astrocytes (mm2)
0.6
0.5
0.4
0.3
0.2
0.1
0.0
Juvenile
Young adult
Old
*
***
***
***
DH
VH

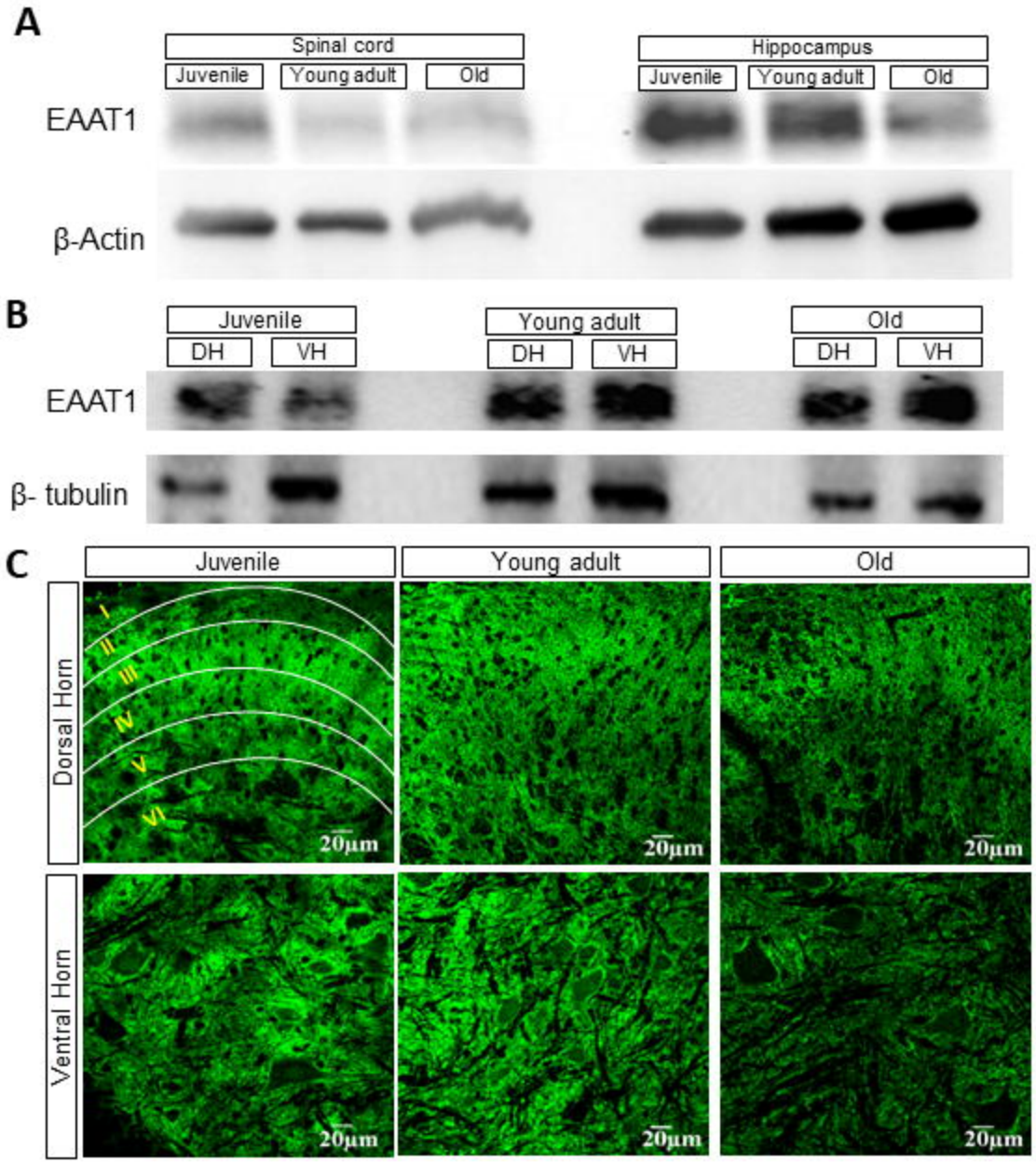
A
Spinal cord
Juvenile
Young adult
Old
Hippocampus
Juvenile
Young adult
Old
EAAT1
β-Actin
B
Juvenile
DH
VH
Young adult
DH
VH
Old
DH
VH
EAAT1
β- tubulin
C
Juvenile
Young adult
Old
Dorsal Horn
Ventral Horn
I
II
III
IV
V
VI
20μm

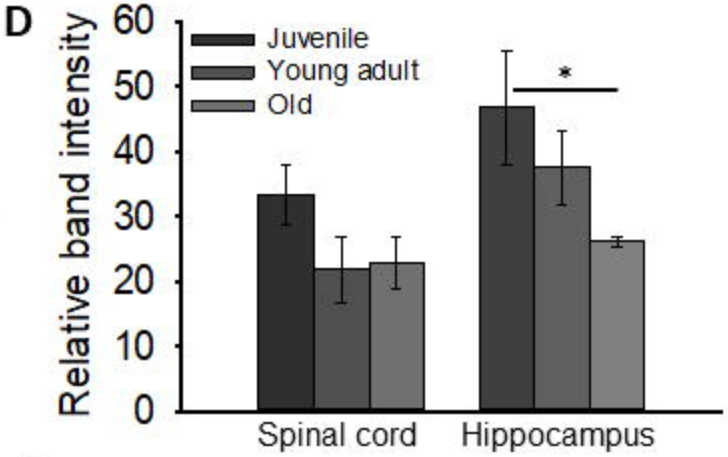
D
Relative band intensity
60
50
40
30
20
10
0
Juvenile
Young adult
Old
*
Spinal cord
Hippocampus

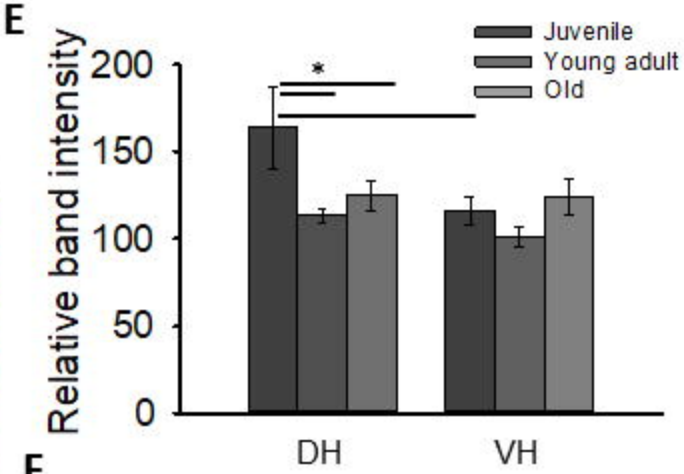
E
Relative band intensity
200
150
100
50
0
Juvenile
Young adult
Old
*
DH
VH

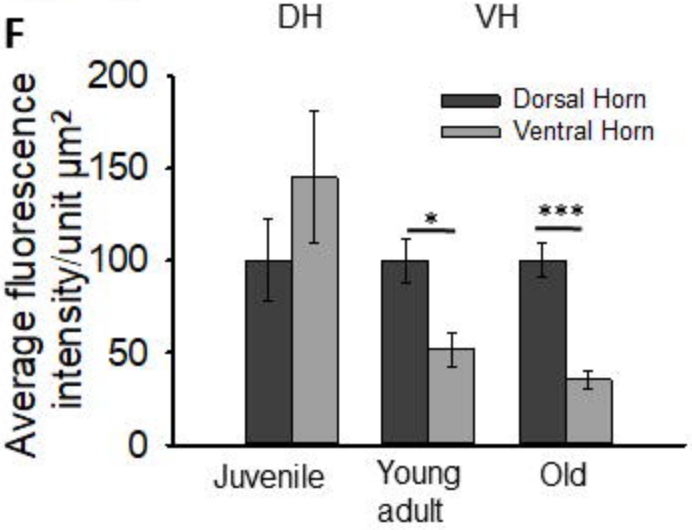
F
Average fluorescence intensity/unit μm²
200
150
100
50
0
Dorsal Horn
Ventral Horn
*
***
Juvenile
Young adult
Old

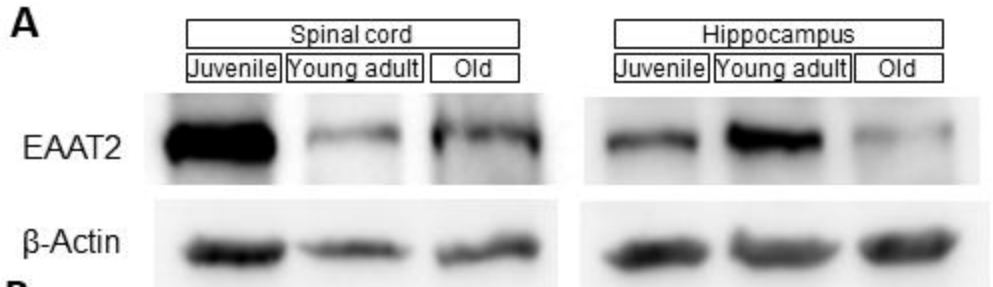
A
Spinal cord
Hippocampus
Juvenile
Young adult
Old
Juvenile
Young adult
Old
EAAT2
β-Actin

B
Juvenile
Young adult
Old
DH
VH
DH
VH
DH
VH
EAAT2
β-tubulin

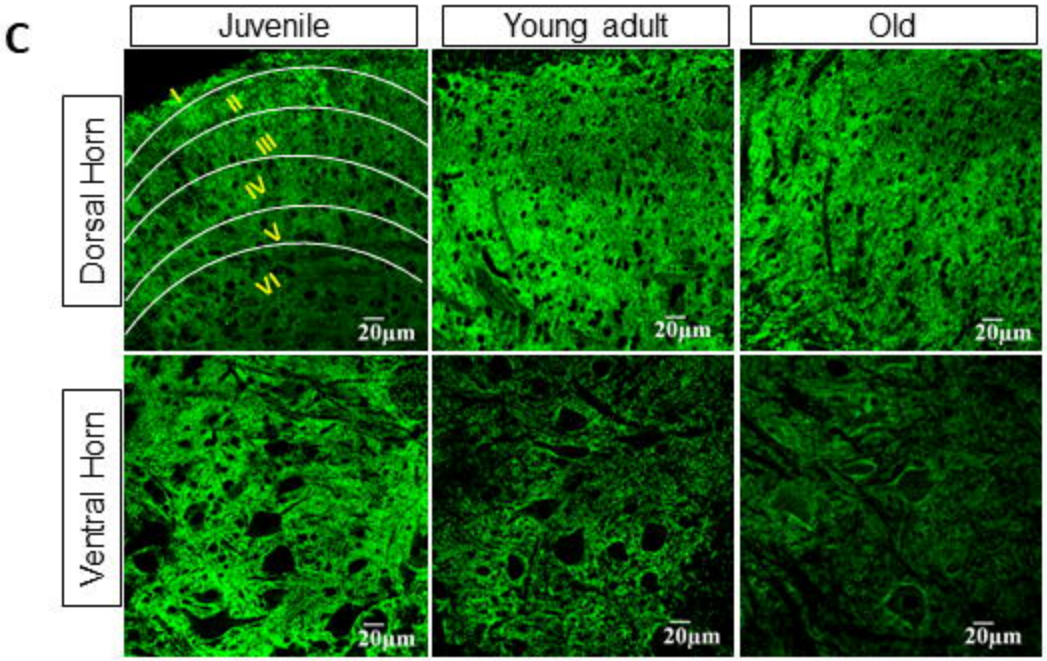
C
Juvenile
Young adult
Old
Dorsal Horn
Ventral Horn
I
II
III
IV
V
VI
20μm

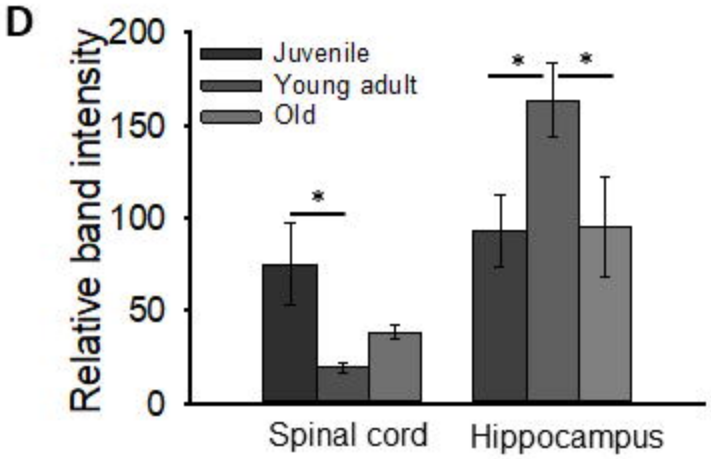
D
Relative band intensity
200
150
100
50
0
Juvenile
Young adult
Old
*
*
*
Spinal cord
Hippocampus

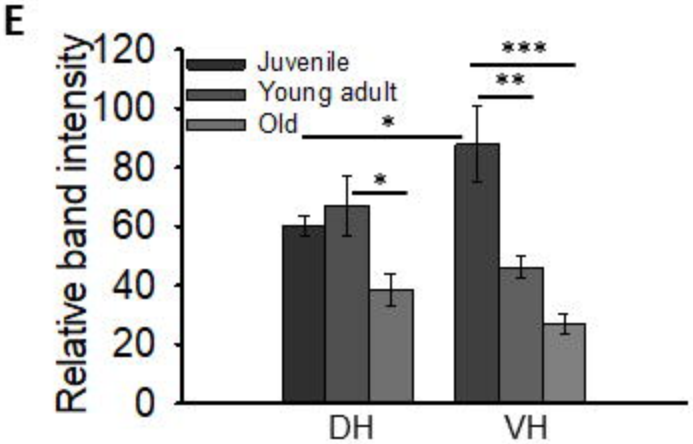
E
Relative band intensity
120
100
80
60
40
20
0
Juvenile
Young adult
Old
*
*
***
**
DH
VH

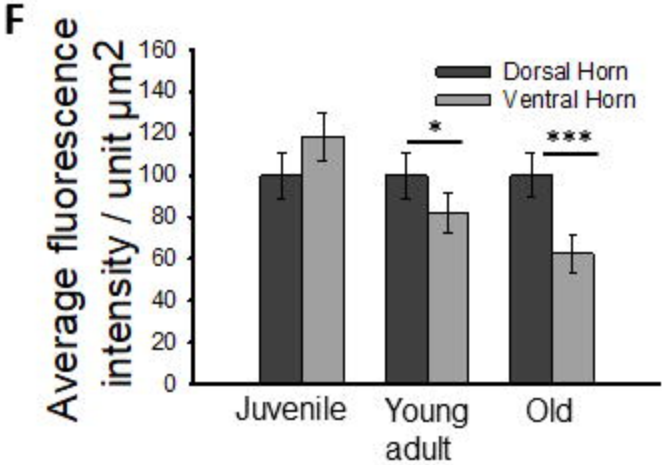
F
Average fluorescence intensity / unit μm2
160
140
120
100
80
60
40
20
0
Dorsal Horn
Ventral Horn
*
***
Juvenile
Young adult
Old

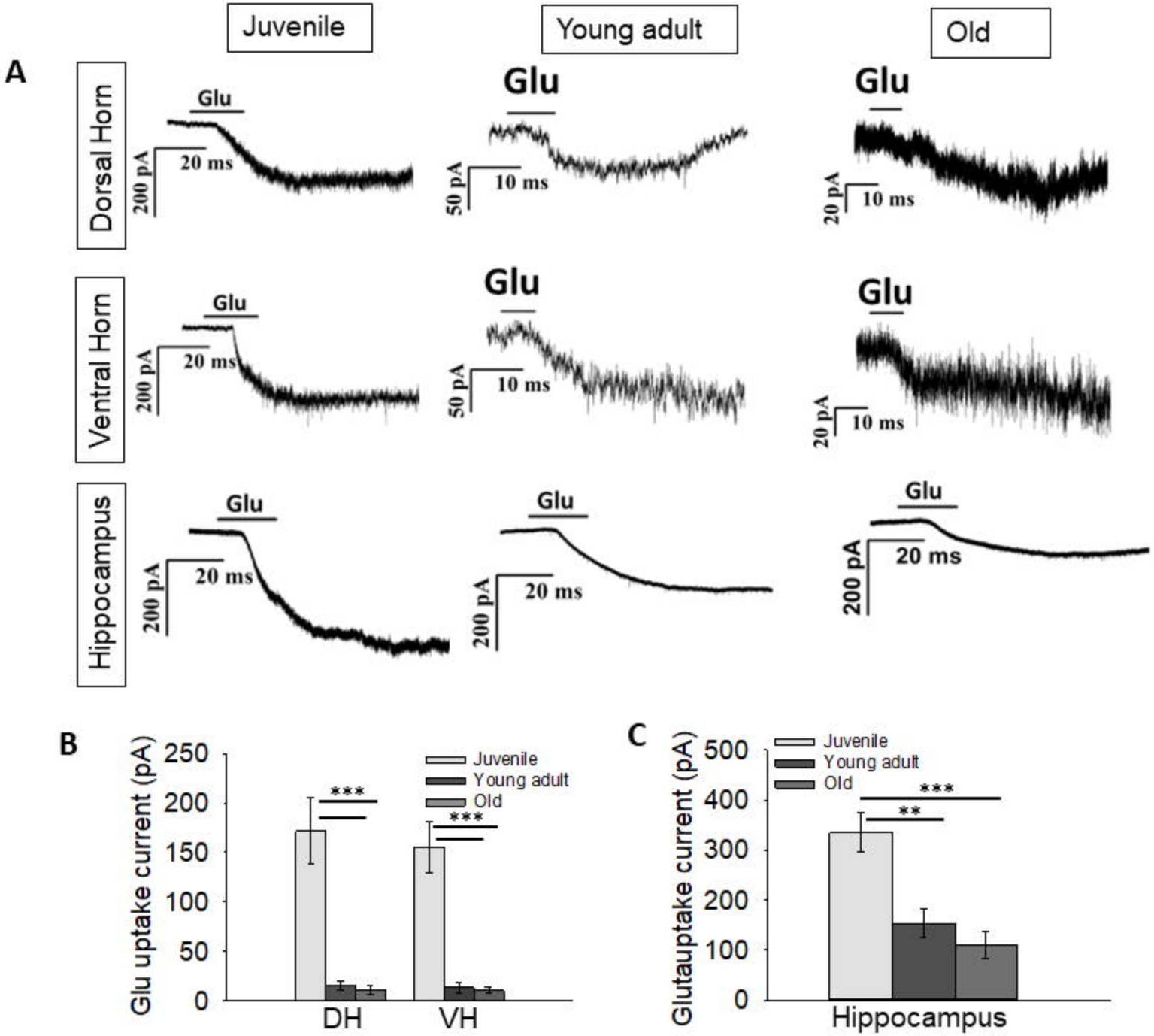
A
Juvenile
Young adult
Old
Dorsal Horn
Ventral Horn
Hippocampus
Glu
200 pA
20 ms
50 pA
10 ms
20 pA
B
Glu uptake current (pA)
250
200
150
100
50
0
Juvenile
Young adult
Old
***
DH
VH
C
Glutauptake current (pA)
500
400
300
200
100
0
**
Hippocampus

Figure 1. Density of astrocytes decreases with aging in of spinal cord. (A) Representative images of immunohistochemistry showing S100β -labelled astrocytes in dorsal horn and ventral horn of spinal cord, in three age groups. White arrows display astrocytes surrounding neuronal cell body. (B) the density of S100β -labelled astrocytes significantly decreased with aging in spinal cord. (C) Density of astrocytes decreased in dorsal horn and ventral horn regions of spinal cord with aging. (D) despite the number of astrocytes going down with age the area acquired by astrocytes increased with age, area acquired by young adult astrocytes was highest. (E) Graph shows same pattern in dorsal horn and ventral horn regions of spinal cord with least area acquired by juvenile astrocytes and maximum area acquired by young adult astrocytes. Data represent the mean ±S.E.M., n= 3-5 rats. (*$P \leq 0.05$; **$P \leq 0.01$; ***$P \leq 0.001$)

Figure 2. EAAT1 glutamate transporter expression decreased with aging in hippocampus of SD rat: (A -B) Representative western blots show EAAT1, and beta-actin/beta-tubulin bands. (C) Confocal image of a transverse section of rat lumbar spinal cord lamination immunostained with EAAT1 astrocytic glutamate transporter. White lines represent boundaries of the dorsal horn laminae. Astrocytes from three age groups were immunostained with EAAT1 to access effect of age in glutamate transporter expression. (D) western blot analysis showed a decline in EAAT1 expression with aging in hippocampus although there was no significant change in EAAT1 expression with age in spinal cord. (E) comparing EAAT1 expression in regions of spinal cord, EAAT1 showed decline in its expression when dorsal horn of young adult and old rats were compared with juvenile rats. Also, the expression of EAAT1 in ventral horn of juvenile rats were less than ventral horn. (F) evaluation of EAAT1 immunofluorescence in regions of spinal cord showed decreased EAAT1 expression in DH of young adult and old rats with no change in juvenile age group. Western blot data represent the mean ±S.E.M. of n=3 rats. IHC data represent the mean ±S.E.M. of n=4 rats. (*$P \leq 0.05$; ** $P \leq 0.01$; ***$P \leq 0.001$)

Figure 3. Most crucial glutamate transporter EAAT2 showed reduced expression with aging in regions of spinal cord. (A-B) western blot images of EAAT1, and beta-actin/beta tubulin bands. (C) immunostaining of astrocytes with EAAT2 transporter indicated the differential laminar expression pattern of transporter with intense expression in lamina II, III and IV of dorsal horn (white lines) especially in young adult and old groups. (D) Spinal cord tissue had highest EAAT2 expression in juvenile age group followed by old and young adult groups. However, the positive control hippocampus portrayed highest EAAT2 levels in young adult rats. (E) The expression of EAAT2 decreased with maturing in both dorsal horn and ventral horn of spinal cord with more prominent decrease in ventral horn. (F) immunofluorescence data showed lower EAAT2 expression in DH higher age groups as compared to VH astrocytes. Western blot data represent the mean ±S.E.M. of n=3 rats. IHC data represent the mean ±S.E.M. of n=4 rats. (*$P \leq 0.05$; **$P \leq 0.01$; ***$P \leq 0.001$)

Figure 4. Glutamate transporter current in hippocampal and spinal astrocytes: (A) Representative astrocytic glutamate uptake current traces in spinal cord and hippocampal astrocytes with age. (B) Bar graph shows huge decline in average glutamate uptake current recorded from astrocytes of dorsal and ventral horn in spinal cord of young adult and old groups. (C) hippocampal astrocytes demonstrated decline in glutamate uptake current with growing age. [Hippocampal astrocytes (n=5-8); 15-30 Days Dorsal horn (n=12); Ventral horn (n=12); 2-3 months and 18-20 months Dorsal horn (n=5); Ventral horn (n=5). Data represented as the mean ±S.E.M. (*$P \leq 0.05$; **$P \leq 0.01$; ***$P \leq 0.001$)